Published in final edited form as:
J Am Coll Cardiol. 2008 September 2; 52(10): 828–835. doi:10.1016/j.jacc.2008.05.040.

Superiority of Biphasic Over Monophasic Defibrillation Shocks is Attributable to Less Intracellular Calcium Transient Heterogeneity

Gyo-Seung Hwang, MD, PhD, **Liang Tang, PhD**, **Boyoung Joung, MD, PhD**, **Norishige Morita, MD, PhD**, **Hideki Hayashi, MD, PhD**, **Hrayr S. Karagueuzian, PhD**, **James N. Weiss, MD**, **Shien-Fong Lin, PhD**, and **Peng-Sheng Chen, MD**

Division of Cardiology, Department of Medicine, Cedars-Sinai Medical Center (GSH, NM, HH), the Departments of Medicine (Cardiology) and Physiology, David Geffen School of Medicine at UCLA (JNW, HSK), Los Angeles, California and the Krannert Institute of Cardiology, Indiana University School of Medicine, Indianapolis, Indiana (LT, BYJ, SFL, PSC)

Abstract

Objectives—To test the hypothesis that superiority of biphasic waveform (BW) over monophasic waveform (MW) defibrillation shocks is attributable to less intracellular calcium (Ca_i) transient heterogeneity.

Background—The mechanism by which BW shocks have a higher defibrillation efficacy than MW shocks remains unclear.

Methods—We simultaneously mapped epicardial membrane potential (Vm) and Ca_i during 6 ms MW and 3/3 ms BW shocks in 19 Langendorff-perfused rabbit ventricles. After shock, the percentage of depolarized area was plotted over time. The maximum (peak) postshock values (VmP and Ca_iP, respectively) were used to measure heterogeneity. Higher VmP and Ca_iP imply less heterogeneity.

Results—The defibrillation threshold was for BW and MW shocks were 288±99 V and 399±155 V, respectively (p=0.0005). Successful BW shocks had higher VmP (88±9 %) and Ca_iP (70±13 %) than unsuccessful MW shocks (VmP 76 %±10, p<0.001; Ca_iP, 57±8 %, p<0.001) of the same shock strength. In contrast, for unsuccessful BW and MW shocks of the same shock strengths, the VmP and Ca_iP were not significantly different. MW shocks more frequently created regions of low Ca_i surrounded by regions of high Ca_i (postshock Ca_i sinkholes). The defibrillation threshold for MW and BW shocks became similar after disabling the sarcoplasmic reticulum with thapsigargin and ryanodine.

Conclusions—The greater efficacy of BW shocks is directly related to their less heterogeneous effects on shock-induced sarcoplasmic reticulum Ca release and Ca_i transients. Less heterogeneous Ca_i transients reduces the probability of Ca_i sinkhole formation, thereby preventing the postshock reinitiation of VF.

Keywords

resuscitation; sarcoplamic reticulum; electrical stimulation; polarity

For correspondence: Peng-Sheng Chen, MD, Krannert Institute of Cardiology, 1801 N. Capitol Ave, E475, Indianapolis, IN 46202. Phone: 317-962-9755. Fax: 310-423-0318 email: chenpp@iupui.edu.

There are no conflicts of interests related to this basic science study.

Biphasic waveform (BW) is more effective than monophasic waveform (MW) in achieving successful defibrillation. The mechanisms underlying the superiority of BW were unclear. One hypothesis is that BW improves defibrillation efficacy by lowering the excitation threshold (1). This hypothesis, however, was not supported by subsequent studies (2,3). Kao et al (4) showed that an electrical stimulus occurring during relative refractory period could induce graded responses and prolong action potential (AP). It is possible that action potential (refractoriness) extension could underlie the mechanisms of defibrillation (5). If so, then BW should be more effective than MW in prolonging the refractoriness. However, Zhou et al (6) showed that the BW shocks prolonged the action potential duration (APD) to a lesser degree than the MW shocks. Efimov et al (7) suggested that the higher defibrillation efficacy of BW may be related to the suppression of virtual electrode-induced phase singularities in the postshock period. In addition to changes of membrane potential, defibrillation shocks also have significant effects on intracellular calcium (Ca_i) transients (8). Hwang et al (9) demonstrated that the heterogeneous distribution of Ca_i during the postshock isoelectric window (10) plays a key role in the defibrillation outcome because the first postshock activation always occurred from a region of low Ca_i surrounded by high Ca_i (Ca_i sinkhole). We hypothesized that MW shocks would be more likely to produce Ca_i sinkholes than BW shocks of similar strengths by creating spatially distinct virtual anodes and cathodes during the shock. Because hyperpolarization may have significantly different effects on the evolution of the Ca_i transient than depolarization, the spatially distinct virtual electrodes during a MW shock may accentuate Ca_i transient heterogeneity and facilitate the formation of Ca_i sinkholes. In contrast, during a BW shock, virtual anode formed during the first half of the shock become virtual cathode during the second half of the shock, and vice versa, producing a balanced effect on sarcoplasmic reticulum (SR) Ca release. This reduces Ca_i transient heterogeneity makes the formation of Ca_i sinkholes less likely. To test this hypothesis, we compared the effects of MW and BW shocks on the 50% probability of successful defibrillation (DFT_{50}) in isolated Langendorff-perfused rabbit ventricles, using dual optical mapping to record epicardial membrane potential and Ca_i simultaneously (11). We found that superiority of BW over MW was due to less Ca_i transient heterogeneity, as hypothesized.

Methods

Surgical Preparation

The study protocol was approved by the Institutional Animal Care and Use Committee. New Zealand white rabbits (N=27) weighing 5.1 0.5 kg were used in this study. The hearts were perfused through aorta with Tyrode solution (NaCl 125, KCl 4.5, NaH_2PO4 1.8, $NaHCO_3$ 24, $CaCl_2$ 1.8, $MgCl_2$ 0.5, and dextrose 5.5 mmol/L, added albumin 100 mg/L in deionized water). S_1 pacing was given to left ventricular (LV) apex. Defibrillation shocks were applied through right ventricular (RV) endocardial and LV patch electrode using direct current shocks.

Optical Mapping

The hearts were stained with Rhod-2 AM and RH237 (Molecular Probes) and excited with laser light at 532 nm (12). In the first 25 hearts, fluorescence was collected using two charge-coupled device (CCD) cameras (Dalsa) covering the same mapped field. We used a grid to calibrate the locations of the field of view of these two CCD cameras. The digital images (128 × 128 pixels) were gathered from the epicardium of the LV (25 × 25 mm^2 area). We acquired 1000 frames continuously for 4 seconds. The actual camera speed was calibrated by the pacing cycle length of the Bloom stimulator. The calibrated frame rate, which varied between 250 frames per second to 400 frames per second, was used for data analyses. For the last 2 hearts, we used Micam Ultima-L dual camera system for data acquisition. There were 100X100 pixels per camera acquiring at 500 frames/s. Cytochalasin D (cyto-D, 5 μmol/L) was added to the perfusate to inhibit motion.

Dual Optical Mapping of MW and BW Shocks

After 8 S_1 paced beats at 300 ms cycle length, fixed duration monophasic (6 ms) and biphasic (3/3 ms) truncated exponential waveform shocks were delivered from a Ventritex HVS-02 defibrillator in 19 hearts. The RV endocardial electrode was cathode and a patch on the LV posterior wall was anode during MW shocks. During BW shocks, the first phase used LV and RV electrodes for anode and cathode, respectively. The polarity switched during the second phase. After VF was induced by shock on T, an up-down algorithm was used to determine the DFT_{50}. We defined the near-threshold shock strengths as shock strengths within 50 V from the DFT_{50} (13).

Effects of Ryanodine and Thapsigargin

We performed 6 additional experiments to test the importance of SR Ca cycling on MW and BW shock defibrillation. The DFT_{50} was estimated before and after 30 min of perfusion with ryanodine 10 μmol/L and thapsigargin 1 μmol/L.

Shock Polarity and APD

We delivered monophasic anodal shocks and cathodal shocks at 160 ms S1-shock coupling intervals to the same defibrillation electrodes in an additional 2 hearts. The S1 pacing cycle length was 350 ms for these 2 studies. The changes of APD throughout the mapped region were then analyzed.

Analysis of Optical Signals

The average fluorescence level ($\bar{F}$) over the entire 1000 frames was first calculated for each pixel. The fluorescent level at different time points on that pixel was then compared with this average. The difference (delta) of the fluorescent level and the average fluorescence ($F-\bar{F}$) was divided by the average fluorescence ($\bar{F}$) to obtain a percentage of change above and below the average fluorescence. Shades of red and blue were used to indicate percentage of change above and below the average fluorescence, respectively, on the ratio maps.

Quantitative Analysis of Postshock Membrane Potential and Ca_i Changes

At each frame after shock, we determined the size (percentage) of the mapped region coded red. By default, the pixel is coded red if its fluorescence level is higher than the average (50%) fluorescence. We also performed the same analyses by coding the pixels red when the fluorescence exceeded (a) 25% average fluorescence and (b) 75% average fluorescence. We then plotted the percentage of frames coded red after defibrillation shocks (time zero) against time. The peak values (VmP and Ca_iP, respectively), and the time from the shock to their peak values (VmPT and Ca_iPT, respectively) were determined for each shock strength.

Previous studies showed that a near-threshold unsuccessful defibrillation shock is usually followed by synchronized repolarization (5), leading to the formation of a quiescent period during which no activation is present (13). In contrast to synchronized repolarization of membrane potential, the postshock Ca_i changes are not synchronized, with some areas showing continued Ca_i decline while the neighboring areas showing persistent Ca_i elevation. A Ca_i sinkhole is formed when a low Ca_i area is completely surrounded by high Ca_i area (9).

Statistical Analysis

All data were presented as means ± SD. Student's paired t tests were used to compare the mean values of VmP, Ca_iP, VmPT and Ca_iPT of the same shock strengths between MW and BW shocks ranged between 200V and 600V. Fisher's exact test was used to compare the frequency of Ca_i sinkhole formation after MW and BW shocks. A P-value of ≤ 0.05 was considered statistically significant.

Results

Unsuccessful MW Shocks and Successful BW Shocks at Equivalent Shock Strengths

The DFT_{50} for MW shocks was higher than with BW shocks (399±155 V vs 288±99 V, P=0.0005). In 12 hearts, we analyzed 33 pairs of shocks at the same strength in which MW shocks resulted in failed defibrillation but BW shocks resulted in successful defibrillation. Figure 1 shows a typical example comparing an unsuccessful MW shock with a successful BW shock at the same intensity. The percent areas of the mapped region with greater than average membrane potential and Ca_i levels are indicated at the top of each map.

The VmP was larger after the BW shock (76%, Panel B2) than the MW shock (66%, Panel A2). The Ca_iP was also larger in BW than in MW (77% in Panel B3 vs 59% in Panel A3). The times between the shock and VmP (VmPT) after MW and BW shocks were 15 ms and 9 ms (Panel A2 and B2), respectively. The times between the shock and the Ca_iP (Ca_iPT) after the MW and BW shocks were 21 ms and 18 ms, respectively, in these episodes (Panel A3 and B3). The time of Ca_i sinkhole formation (white arrow) was 45 ms for the MW and was 57 ms for BW shock (Panels 4 and 5, respectively). For all 33 pairs of MW and BW shocks at the same shock strength, Ca_i sinkholes were observed in 100 % of the unsuccessful MW shocks and in 64 % of the successful BW shocks ($p<0.001$). As reported in a previous study (9), the Ca_i sinkholes were not observed in type A successful defibrillation. In 13 episodes, the first postshock activation originated from the Ca_i sinkholes within the mapped region (9). The VmP (76 %±10 vs. 88±9 %, $p<0.001$) and Ca_iP (57±8 % vs. 70±13 %, $p<0.001$) during the isoelectric window were lower after unsuccessful MW than successful BW shocks. The VmPT was 16±6 ms vs. 10±3 ms ($P<0.001$) and Ca_i PT was 23±6 ms vs 18±4 ms ($P< 0.001$) after MW and BW shocks, respectively. Figure 2 summarizes these findings.

These results were independent of the threshold fluorescence levels used to code the pixels red. When the threshold level was 75%, the VmP for MW and BW was 25±10% vs 32±16%, respectively ($p=0.015$) and the Ca_iP was 9±3% and 12±6%, respectively ($p<0.001$). When the threshold level was 25%, the VmP for MW and BW was 99±1% and 100±1% respectively ($p<0.001$) and the Ca_iP was 93±4% and 95±4%, respectively ($p<0.001$).

Unsuccessful BW and Unsuccessful MW Shocks at Equivalent Shock Strengths

We analyzed membrane potential-Ca_i dynamics during the postshock isoelectric window in 58 pairs (19 rabbits) of voltage-matched BW and MW shocks (354±106 V) near the DFT_{50} that failed to terminate VF. In contrast to the data presented in the previous paragraph, the VmP (78±9 % vs. 79±10 %) and Ca_iP (57±7 % vs. 58±7 %) during the isoelectric window were not different after failed MW and BW shocks, respectively. However, the isoelectric window was longer after BW shocks than MW shocks (65±11 ms vs 56±10 ms, respectively, $P< 0.001$). The VmPT was 16±6 ms vs. 11±4 ms ($P< 0.001$) and for Ca_i PT it was 22±7 ms vs 17±6 ms ($P<0.001$) after MW and BW shocks, respectively. Figure 3 shows these findings at different MW and BW shock strengths.

We compared 18 pairs of successful defibrillation induced by MW and BW shocks of equal strength (275±90 V). We found 7 of the 18 episodes in MW shocks and 3/18 (P=NS) in BW shocks were type B successful defibrillation (10).

Ca_i Sinkholes After MW and BW Shocks

We analyzed 29 pairs (MW vs. BW) of unsuccessful defibrillation episodes in which the earliest postshock focal activation originated from the Ca_i sinkholes. We found that the Ca_i sinkholes emerged significantly ($P = 0.02$) earlier after MW shocks (29±10 ms) than after BW shocks (35±11 ms) in all 29 episodes analyzed. For both MW and BW shocks, the successful

defibrillation was associated with larger VmP and Ca_iP than failed defibrillation (Table 1). After ryanodine and thapsigargin, the DFT_{50} for MW and BW shocks (232±42 V and 182±20 V, P=0.02) decreased to 165±43 V and 160±43 V (p=0.76), respectively.

Action potential and Ca_i Transient Characteristics After MW versus BW Shocks

Figure 4A shows that when a shock was delivered at a long coupling interval (300 ms) when repolarization was complete, MW and BW shocks had similar effects on the action potential and Ca_i transient. However, when shocks were delivered at a shorter coupling interval (160 ms) during the relative refractory period (most frequently associated with the induction of VF), BW shocks caused less prolongation of the Ca_i transient duration than MW shocks (Figure 4B). Table 2 summarizes the results of all hearts studied. The single pixel analyses were performed by selecting a single representative pixel from the center of the mapped region. The summed fluorescence over the entire mapped region was also analyzed. We found that at the coupling interval of 160 or 140 ms, the duration of the Ca_i transient (at 70% return to baseline) was significantly shorter and more homogeneous for BW shocks than for MW shocks. The single pixel analyses showed the same trend.

Greater APD Prolongation at Virtual Anode than Virtual Cathode

To further characterize the effects of virtual anodes versus cathodes on APD, we compared monophasic anodal and cathodal shocks at an S1-shock interval of 160 ms in an additional two hearts. Figure 5A shows that both anodal and cathodal shocks prolonged APD at the site indicated by the arrows in Figure 5B. Figure 5B shows the formation of virtual anode and virtual cathode (arrows) during the anodal and cathodal shocks, respectively, on the epicardium near the RV endocardial electrodes. To compare the effects of shocks on APD, we subtracted the prolonged APD after the anodal shock (APD2) from that after the cathodal shock at all pixels. Figure 5C shows that in the region of the virtual electrodes there was greater prolongation of APD at anodal sites than at cathodal sites, whereas in regions surrounding the virtual electrodes, the opposite occurred. The maps of a second heart showed the same finding.

Discussion

In the present study, we present evidence showing that the greater efficacy of BW shocks is associated with their less heterogeneous effects on shock-induced SR Ca release and Ca_i transients.

Postshock Heterogeneity and the Shock Outcome

We quantified the heterogeneity by VmP and Ca_iP. A higher peak value implies a greater ability for shocks to depolarize Vm and elevate SR Ca release everywhere, reducing the Vm dispersion and the likelihood of Ca_i sinkhole formation. Using this method, we found that the successful BW shocks resulted in less heterogeneous postshock Vm and Ca_i distributions than unsuccessful MW shocks of the same strength. When both MW and BW shocks failed, there were no consistent differences between heterogeneity parameters. These findings indicate that successful defibrillation is associated with less postshock heterogeneity.

Sources of Shock-Induced Heterogeneity

We found that virtual anode sites were followed by larger APD prolongation than at virtual cathode sites, consistent with the hypothesis that hyperpolarization at virtual anodes increased the driving force for Ca entry through L-type Ca channels, triggering additional SR Ca release. The increased Ca_i then prolonged APD by potentiating inward Na-Ca exchange current, consistent with positive Ca_i-APD coupling (14). At virtual cathode sites, APD and Ca_i were also increased by further membrane depolarization, perhaps by reactivating recovered L-type

Ca channels, but the effects were more modest. These differential APD prolongation effects were observed only in late phase 2 or phase 3 of the AP, but not after full repolarization. During fibrillation, the effects of virtual cathodes and anodes on APD and Ca_i transient duration are also likely to be variable depending on local repolarization state relative to the timing of the shock. This makes it unlikely that Ca_i sinkholes would reliably form at virtual anodes or cathodes. Nevertheless, the greater efficacy of BW shocks at preventing or delaying Ca_i sinkhole formation is probably best attributed to an overall more balanced effect on the APD and the Ca_i transient, since regions that are virtual cathodes during the first half of the shock become virtual anodes during the second half of the shock, and vice versa. That is, the switching between anode and cathode half way through the shock should partially neutralize the heterogeneous effects of virtual electrodes on APD and Ca_i, hence reducing postshock heterogeneity and improving defibrillation efficacy.

Comparison With Previous Studies

Raman et al (15) have studied the effects of shocks on Ca_i, and found that the effects of shocks depend on the timing of application. Their analyses focused on the changes of Ca_i during the shock. However, Figure 2 of that manuscript showed a greater magnitude of Ca_i elevation and APD prolongation at virtual anode site than at virtual cathode site. Figure 5 of the present report is consistent with their findings. Yabe et al (16) gave shocks 300 ms after the last paced beat. Pacing studies before and after shocks showed BW caused less conduction block than MW. Because we found no differences of Ca_i transients after BW shocks and MW shocks given 300 ms after the last paced beat, Yabe's findings cannot be explained by the changes of Ca_i transients.

Limitations

Due to the existence of transmural heterogeneity (17), the changes in Vm and Ca_i in the intramural or subendocardial layers of the ventricles might be different than that on the epicardium. A limitation of our study is that we were not able to map the shock effects below the epicardium to determine the transmural changes of Vm and Ca_i. It is possible that the mitochondrial Ca signal influenced the recording of Ca transient. However, previous studies showed that Rhod-2 was primarily trapped in the cytosol and not in subcellular organelles such as mitochondria (11).

Summary and Implications

BW shocks result in less spatial heterogeneity of Ca_i and delayed formation of Ca_i sinkholes, which in turn leads to delayed onset of the first postshock activation and longer isoelectric window as compared with MW shocks. The delayed emergence of the first postshock activation provides greater recovery time for the ventricles, thereby ensuring a higher safety factor for propagation without wavebreak. This sequence of events explains the mechanisms by which BW is more effective than MW in achieving ventricular defibrillation. We conclude that the greater efficacy of BW shocks is directly related to their less heterogeneous postshock Ca_i transient distribution, thus reducing the probability of Ca_i sinkholes formation and VF reinitiation.

Acknowledgements

We thank Avile McCullen, Lei Lin, Elaine Lebowitz and Sandra Owens for their assistance.

This study was supported by the NIH Grants P01 HL78931, R01 HL78932, 58533, 71140, University of California Tobacco Related Disease Research Program (14IT-0001); American Heart Association Grant-in-Aid, Western States Affiliate (0255937Y and 0555057Y), National Scientist Development Grant (0335308N), Established Investigator Award (#0540093N), Kawata, Laubisch, Price and Medtronic-Zipes Endowments, and a Chun Hwang Fellowship for Cardiac Arrhythmia Honoring Dr Asher Kimchi, Los Angeles, Calif. Medtronic, St Jude and Cryocath have donated

equipment to our research laboratory. Dr Chen is a consultant to Medtronic Inc. However, this paper did not include any data on commercial products or advocate off-label use of drugs or equipment.

Reference List

1. Jones JL, Jones RE, Balasky G. Improved cardiac cell excitation with symmetrical biphasic defibrillator waveforms. Am J Physiol 1987;253:H1418–H1424. [PubMed: 3425743]
2. Wharton JM, Richard VJ, Murry CE, et al. Electrophysiological effects of monophasic and biphasic stimuli in normal and infarcted dogs. Pacing Clin Electrophysiol 1990;13:1158–72. [PubMed: 1700392]
3. Daubert JP, Frazier DW, Wolf PD, Franz MR, Smith WM, Ideker RE. Response of relatively refractory canine myocardium to monophasic and biphasic shocks. Circulation 1991;84:2522–38. [PubMed: 1959202]
4. Kao CY, Hoffman BF. Graded and decremental response in heart muscle fibers. Am J Physiol 1958;194:187–96. [PubMed: 13559448]
5. Dillon SM. Optical recordings in the rabbit heart show that defibrillation strength shocks prolong the duration of depolarization and the refractory period. Circ Res 1991;69:842–56. [PubMed: 1873877]
6. Zhou X, Knisley SB, Wolf PD, Rollins DL, Smith WM, Ideker RE. Prolongation of repolarization time by electric field stimulation with monophasic and biphasic shocks in open-chest dogs. Circ Res 1991;68:1761–7. [PubMed: 2036724]
7. Efimov IR, Cheng Y, Yamanouchi Y, Tchou PJ. Direct evidence of the role of virtual electrode-induced phase singularity in success and failure of defibrillation. J Cardiovasc Electrophysiol 2000;11:861–8. [PubMed: 10969748]
8. Fast VG, Ideker RE. Simultaneous optical mapping of transmembrane potential and intracellular calcium in myocyte cultures. J Cardiovasc Electrophysiol 2000;11:547–56. [PubMed: 10826934]
9. Hwang G-S, hayashi H, Tang L, et al. Intracellular calcium and vulnerability to fibrillation and defibrillation in Langendorff-perfused rabbit ventricles. Circulation 2006;114:2595–603. [PubMed: 17116770]
10. Chen P-S, Shibata N, Dixon EG, et al. Activation during ventricular defibrillation in open-chest dogs. Evidence of complete cessation and regeneration of ventricular fibrillation after unsuccessful shocks. J Clin Invest 1986;77:810–23. [PubMed: 3949979]
11. Choi BR, Salama G. Simultaneous maps of optical action potentials and calcium transients in guinea-pig hearts: mechanisms underlying concordant alternans. J Physiol 2000;529(Pt 1):171–88. [PubMed: 11080260]
12. Omichi C, Lamp ST, Lin SF, et al. Intracellular Ca dynamics in ventricular fibrillation. Am J Physiol Heart Circ Physiol 2004;286:H1836–H1844. [PubMed: 14704235]
13. Wang NC, Lee M-H, Ohara T, et al. Optical mapping of ventricular defibrillation in isolated swine right ventricles: demonstration of a postshock isoelectric window after near-threshold defibrillation shocks. Circulation 2001;104:227–33. [PubMed: 11447091]
14. Sato D, Shiferaw Y, Qu Z, Garfinkel A, Weiss JN, Karma A. Inferring the cellular origin of voltage and calcium alternans from the spatial scales of phase reversal during discordant alternans. Biophys J 2007;92:L33–L35. [PubMed: 17172300]
15. Raman V, Pollard AE, Fast VG. Shock-induced changes of Ca(i)2+ and Vm in myocyte cultures and computer model: Dependence on the timing of shock application. Cardiovasc Res 2007;73:101–10. [PubMed: 17134687]
16. Yabe S, Smith WM, Daubert JP, Wolf PD, Rollins DL, Ideker RE. Conduction disturbances caused by high current density electric fields. Circ Res 1990;66:1190–203. [PubMed: 2335021]
17. Antzelevitch C. Heterogeneity and cardiac arrhythmias: an overview. Heart Rhythm 2007;4:964–72. [PubMed: 17599687]

Abbreviations and Acronyms

APD

action potential duration

BW
biphasic waveform

Ca_i
intracellular calcium

Ca_iP
the peak (maximum) area showing higher than average Ca_i after shock

Ca_iPT
time from shock to the Ca_iP

DFT_{50}
shock strength associated with 50% probability of successful defibrillation

$\bar{F}$
The average fluorescence level

SR
sarcoplasmic reticulum

VmP
the peak (maximum) area showing simultaneous depolarization of the membrane potential after shock

VmPT
time from shock to the VmP

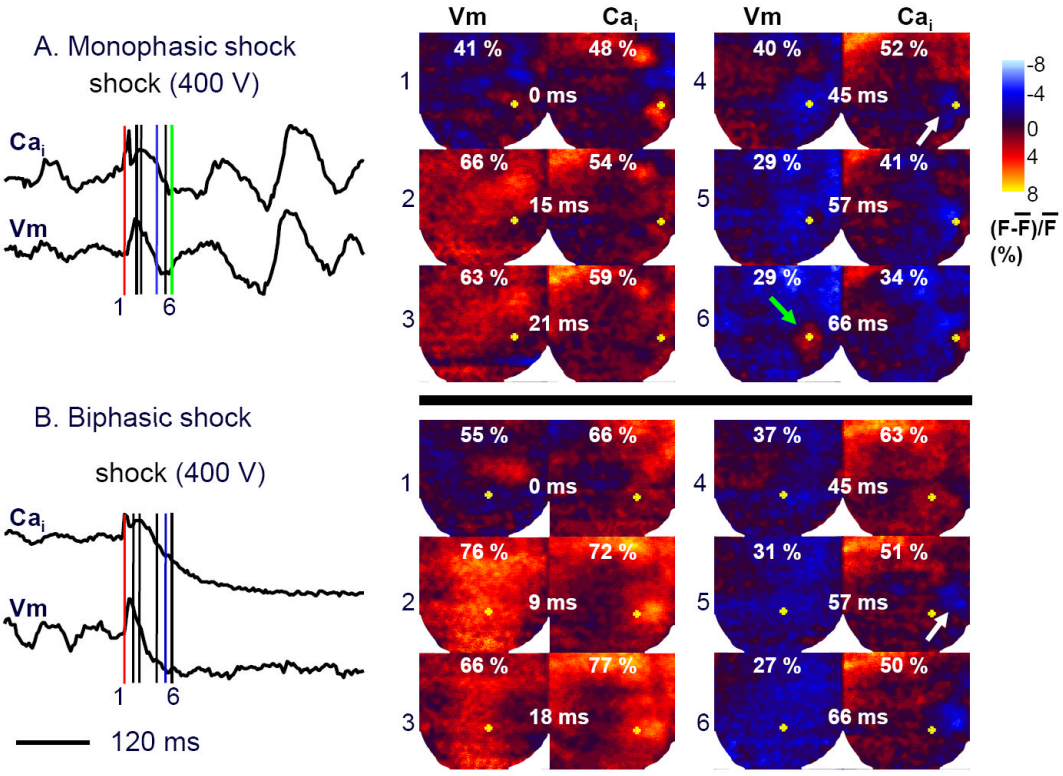

Figure 1. Dual optical mapping of failed defibrillation with MW and successful defibrillation with BW shocks

Left panels of A and B show the time course of the average fluorescence of the entire mapped region following a MW (upper trace) or BW shock (lower trace). Right color panels show fluorescence intensity snapshots after a failed shock (400 V) delivered at 0 ms. Red, blue and green line segments indicate the time of shock, the time of Ca_i sinkhole formation and the end of the isoelectric window, respectively. The yellow dots on Vm maps are at the same location as the yellow dots on the Ca_i maps.

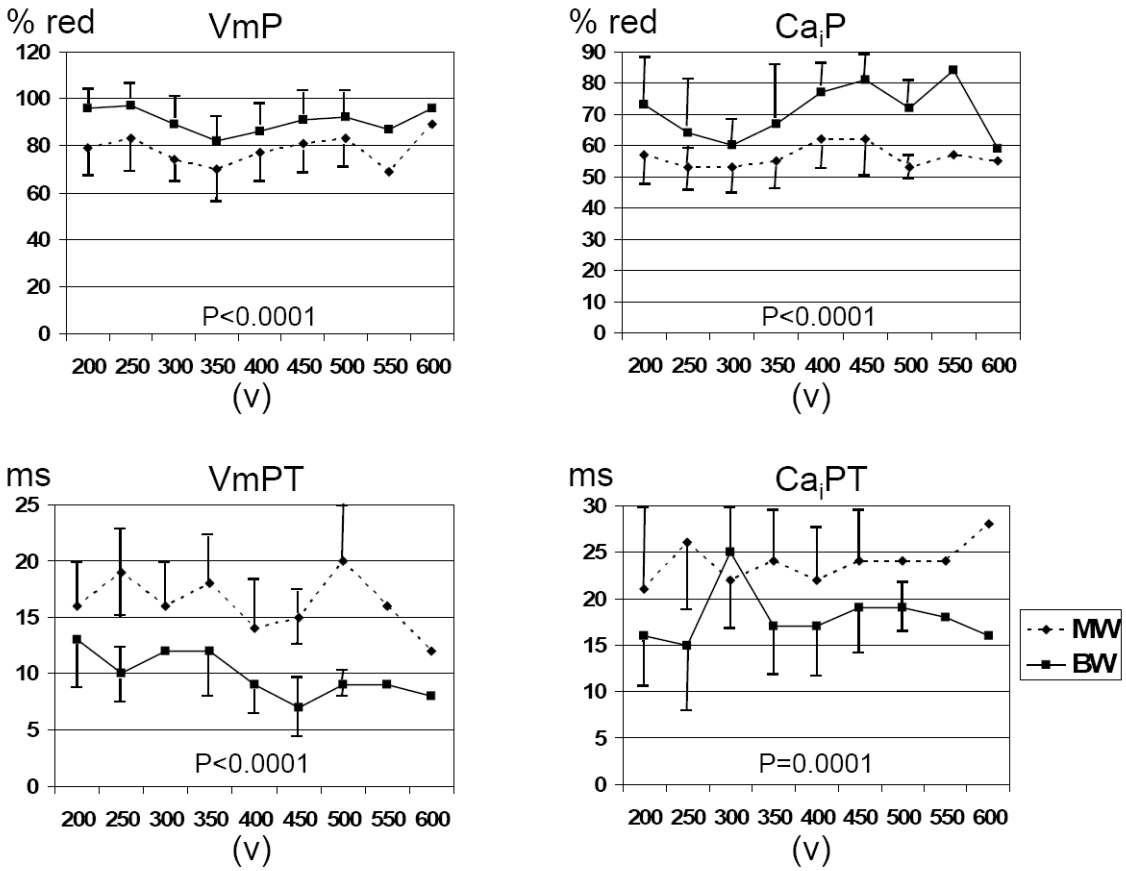

Figure 2. Comparison between successful BW and unsuccessful MW shocks of the same strength

There were significant differential effects of MW and BW shocks on VmP and Ca_iP, VmPT and Ca_iPT.

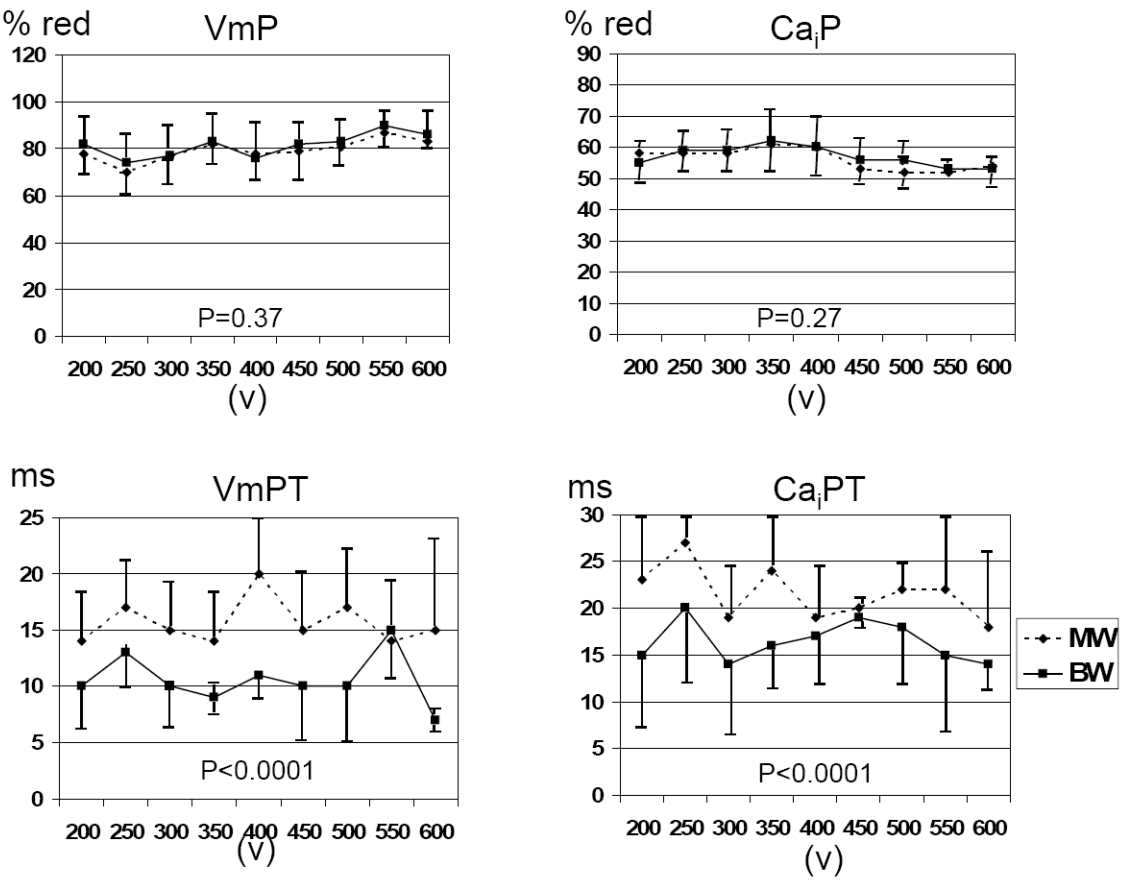

Figure 3. Comparison between unsuccessful BW and unsuccessful MW shocks of the same strength

There were no differences of VmP and Ca_iP for MW and BW shocks of the same strength. However, there were significant differences of VmPT and Ca_iPT.

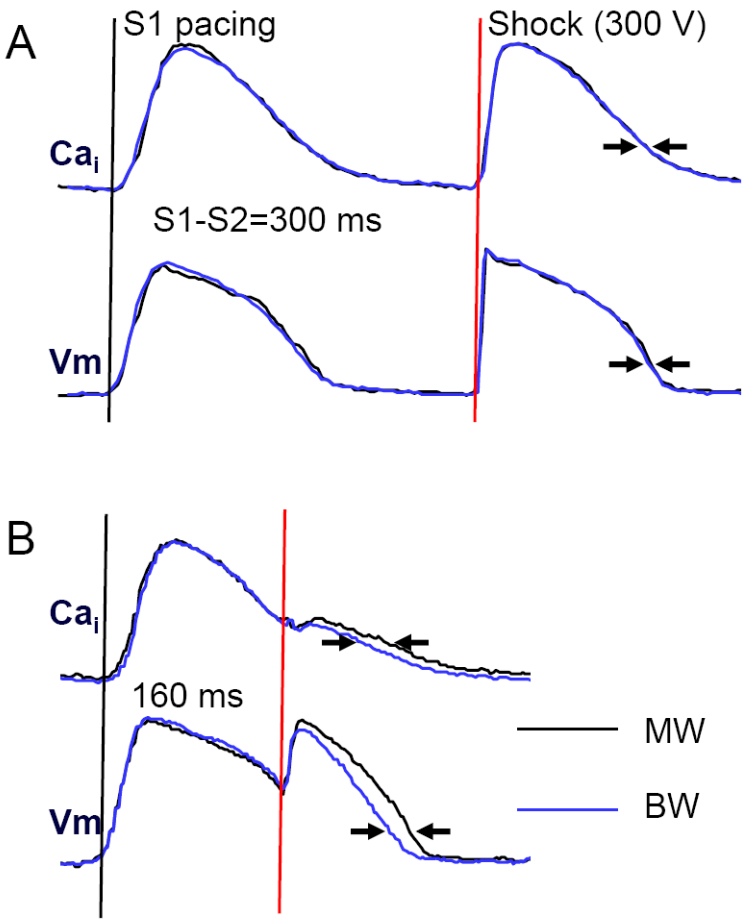

Figure 4. The change of APD_{70} and Ca_iD_{70} after MW and BW shocks delivered at different coupling intervals

MW and BW shocks resulted in different APD_{70} and Ca_iD_{70} when the coupling interval was short (160 ms), but not when the coupling interval was 300 ms. The optical signals were generated by averaging the fluorescence of the entire mapped region.

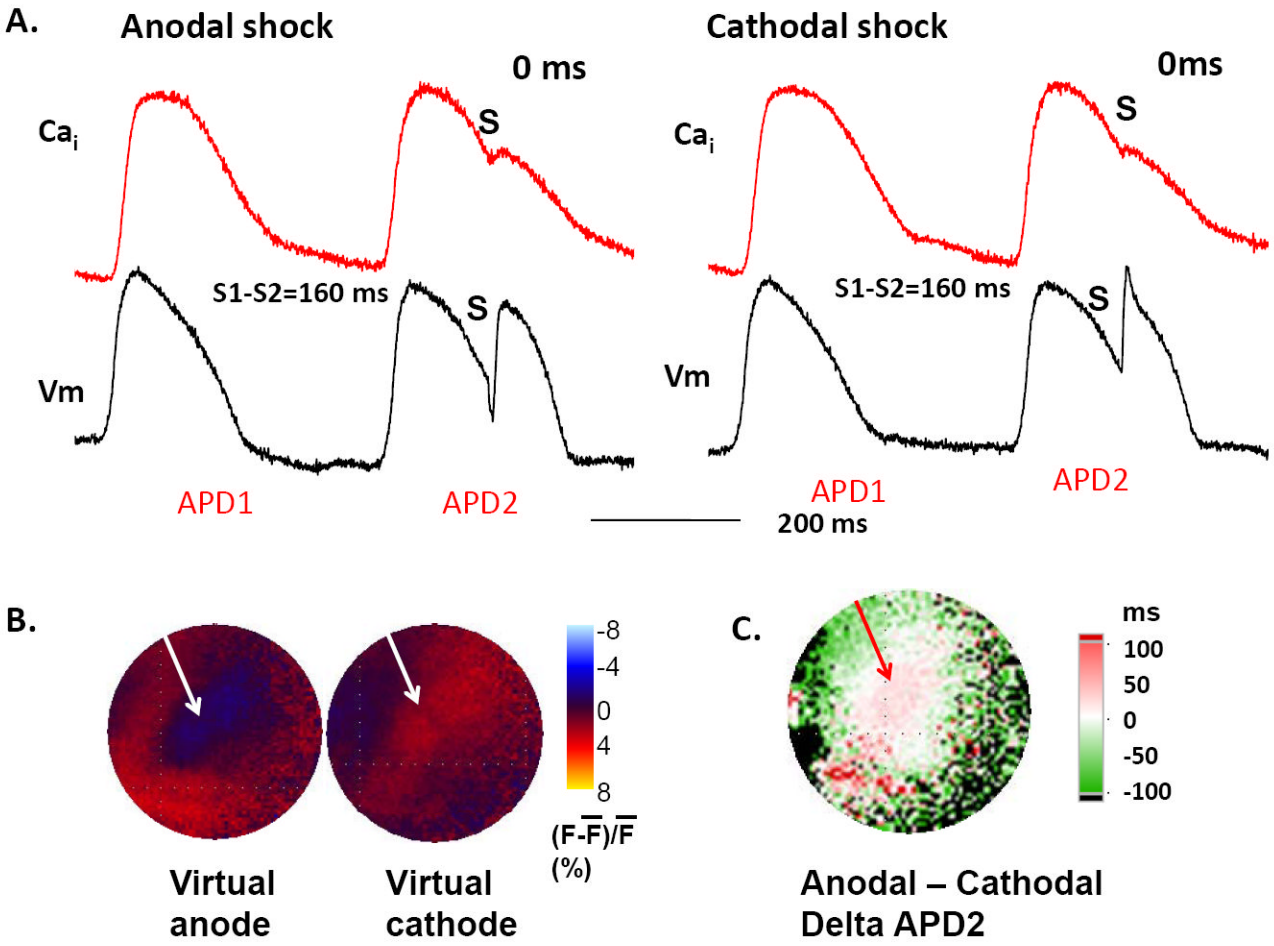

Figure 5. Delta APD and Ca_i transient duration (CaT) maps and virtual electrode distribution during a 300 V monophasic shock

A shows the effects of shock (S) on the optical recordings at the sites indicated by arrows in B. B shows virtual anode (blue) and virtual cathode (red) during the monophasic shocks. C shows the difference (delta) map between the APD of the post-shock beat (APD2) constructed by subtracting APD2 of a cathodal shock by APD2 of an anodal shock. White to red colors indicate longer APD at the virtual anode than at virtual cathode, whereas the difference is reversed at surrounding sites.

Table 1

Effects of shock strength

	MW fail	MW success	P-value	BW Fail	BW success	P-value
Voltage (V)	268±98	396±149		223±79	318±96	
VmP (%)	78±14	93±7	0.002	76±10	91±7	<0.001
VmPT (ms)	19±9	14±4	0.03	12±4	9±2	0.01
Ca_iP (%)	53±5	72±13	<0.001	54±6	68±12	<0.001
Ca_iPT (ms)	27±9	21±4	0.03	21±6	17±5	0.04
Time from shock to Ca_i sink hole (ms)	33±10	47±12	0.03	24±11	48±16	0.02

Table 2

Vm and Ca_i changes Induced by Shock on T

	Single Representative Pixel				Summed Fluorescence Analyses			
	APD_{70} (ms)		Ca_{i70} (ms)		APD_{70} (ms)		Ca_{i70} (ms)	
CI	MW	BW	MW	BW	MW	BW	MW	BW
300 ms	164±23	163±28	167±23	165±21	148±8	147±12	151±13	151±11
180 ms	256±45	261±46	253±43	256±41	270±38	269±34	266±42	265±41
160 ms	210±33	206±32	204±35	191±44*	214±36	208±34*	204±31	197±30*
140 ms	195±33	189±42	182±24	177±21*	186±18	177±21*	192±19	185±20*

P< 0.05 compared with MW

BW, biphasic waveform; CI, coupling interval; MW, monophasic waveform

Ca_{i70}, duration of the Ca_i transient between the onset and 70% return to baseline.

APD_{70}, APD between phase 0 and 70% repolarization.